J. Physiol. (1976), **254**, *pp.* 607–638
With 12 *text-figures*
Printed in Great Britain

MEMBRANE CURRENTS OF THE TUNICATE EGG UNDER THE VOLTAGE-CLAMP CONDITION

BY HARUMASA OKAMOTO,* KUNITARO TAKAHASHI AND MITSUNOBU YOSHII

From the Department of Neurophysiology, Institute of Brain Research, School of Medicine, University of Tokyo, Tokyo, Japan

(*Received 6 February 1975*)

SUMMARY

1. Ionic currents of the egg membrane of a certain tunicate, *Halocynthia roretzi* Drashe, were studied by the voltage-clamp technique.

2. The membrane depolarization beyond -55 mV in standard artificial sea water induced mainly transient inward current and slight outward currents, when the holding potential was kept at -90 mV.

3. The transient inward current was composed of two components; the major one showed a faster time course, a more negative critical level of about -55 mV, and a reversal potential around $+60$ mV and the minor one showed a slower time course, a less negative critical level of -10 mV, and no definite reversal potential.

4. The major component became maximum at about -25 mV with the peak time of 6–9 msec at 15° C, and the maximum currents ranged from 0·5 to $1{\cdot}5 \times 10^{-5}$ A/cm^2.

5. The major component of the inward current was abolished by the replacement of Na with choline or Tris or Cs ions, while it was almost unaltered by the replacement with Li. The minor component was independent of Na concentration in the external solution.

6. This major component showed the activation and inactivation identical with those of Na current of other excitable membranes. A conditioning depolarization over -90 mV inactivated the Na current and the half inactivation of the major inward current was obtained by a conditioning pulse to -56 mV, when the pulse duration was 400 msec and the temperature was at 15° C.

* On leave from Department of Neurochemistry, Institute of Brain Research, School of Medicine, University of Tokyo, Tokyo, Japan.

7. The time course of the Na current was formulated with m and h parameters in the following equations:

$$i_{Na} = \bar{g}_{Na}(E_m - E_{Na})m^2h \fallingdotseq \bar{g}_{Na}(E_m - E_{Na})m_\infty^2(1 - e^{-t/\tau_m})^2e^{-t/\tau_h};$$

$$m = m_0 + (m_\infty - m_0)(1 - e^{-t/\tau_m}),$$

$$h = h_\infty + (h_0 - h_\infty)e^{-t/\tau_h}.$$

8. The kinetic parameters τ_m and τ_h of egg Na current were calculated and compared with those of the squid axon. The potential dependence of τ_m and τ_h was almost identical with that of the axon, but the absolute values of both τ_m and τ_h were ten- to twentyfold larger than those of the axon in any range of the membrane potential.

9. The temperature dependence of the kinetic parameters τ_m, τ_h and of the chord conductance $\bar{g}_{Na}$ was studied. The Q_{10}'s for τ_m and τ_h were both 4·0, while the Q_{10} for $\bar{g}_{Na}$ was 2·0 in the temperature range from 5 to 20° C.

10. The outward and inward rectifying conductances of egg membrane were remarkably activated at the potential level above +100 mV and below −70 mV respectively in standard artificial sea water. Both increased currents were subsequently subject to inactivation.

11. It was suggested that Na, Ca, K inward rectifying and K outward rectifying conductances all exist separately in the egg cell membrane and the Na current was essentially identical with that through the Na channel in other excitable membranes.

INTRODUCTION

It was reported that Na and Ca action potentials could be evoked in the tunicate egg cell membrane even before fertilization (Miyazaki, Takahashi & Tsuda, 1972, 1974). It was inferred that those Na and Ca components of the membrane currents had essentially the same properties as those through the 'Na' and 'Ca channels' found in the excitable membranes and that both Na and Ca permeabilities found in the egg cell membranes were transferred successively during the development until one of them was finally selected to produce Na or Ca spikes in the fully differentiated excitable tissues, such as Ca spikes in the striated muscles of the larval tail (Miyazaki *et al.* 1972).

The egg action potential was usually a form of an 'off-response' at the low resting potential of +5 to −10 mV and even when a high resting potential of −70 mV was obtained by the presence of large Ca concentration of 100 mM in the saline, it showed an extremely long plateau, of the order of several seconds, during the falling phase. It was assumed that the poorly developed K delayed rectification in the egg membrane was mainly

reponsible for prolongation of the falling phase, while the time course of Na and Ca currents had the comparable kinetic parameters to those of the excitable membrane (Takahashi, Miyazaki & Kidokoro, 1971; Miyazaki *et al.* 1974*a*). However, it might be expected that the modes of Na and Ca permeation in the egg membrane are significantly different from those of other excitable membranes such as axonal membrane of the squid (Hodgkin, 1958) or the muscle cell membrane of the crustacean (Hagiwara & Naka, 1964).

In the present and succeeding papers (Okamoto, Takahashi & Yoshii, 1976), the voltage-clamp technique was applied to analyse the membrane currents of the tunicate egg cell and it was confirmed that, even in the undifferentiated membrane such as egg cell membrane, Na and Ca currents had fast kinetic properties, as found in other excitable membranes and K outward-going rectification was present, though its amount was scarce.

METHODS

The unfertilized eggs of *Halocynthia roretzi* were exclusively used in the present experiments. The collection of the animals and the methods of spawning and preparing the eggs were described previously (Miyazaki *et al.* 1974*a*).

The egg without the follicular envelope was placed in the centre of a shallow hole, with a diameter two times that of an egg and with a depth, 0·5–0·7 times egg-diameter, dug on the soft transparent silicon seat (Toray Silicon SH 1840K) covering the floor of a Lucite chamber. Other fixed points of the egg were those at which two micro-electrodes were penetrated across the membrane.

The methods of penetrating the eggs, exchanging the bathing solution, and cooling the solutions were described previously (Miyazaki *et al.* 1974*a*). The bath temperature was controlled by a thermoelectric device at a desired level from 5 to 25° C. The bath volume was 2·5 ml. and 7 min was sufficient for more than 99 % exchange of the solutions by flow rate at 3 ml./min. The ionic compositions of the various artificial sea waters (ASW), used in the present experiments, are listed in Table 1. The total ion concentration of ASWs were all the same except that of Na-free ASW, Tris. Therefore, calculation of ion activities is not given. The effects of tetrodotoxin used were checked by the abolition of the action potential in the frog sciatic nerve.

TABLE 1. Ionic composition of the artificial sea water (m-mole/l.)

ASW	Na	K	Ca	Mg	Cl	Choline,	Tris,	Mn^{2+}	*X**
Standard	460	10	10	50	590	—	—	—	—†
Na-free, choline	—	10	10	50	590	460	—	—	—†
Na-free, Tris	—	10	10	50	498	—	552	—	—
X ASW	—	10	10	50	590	—	—	—	460†
Mn ASW	460	10	—	50	590	—	—	10	—†

* *X* is a monovalent cation; Li, Cs, Rb or K.

† 10 mM Tris HCl, pH 7·8, was added in each ASW.

If the intermediate concentration of Na were needed, std ASW and Na-free were mixed in appropriate volume ratio.

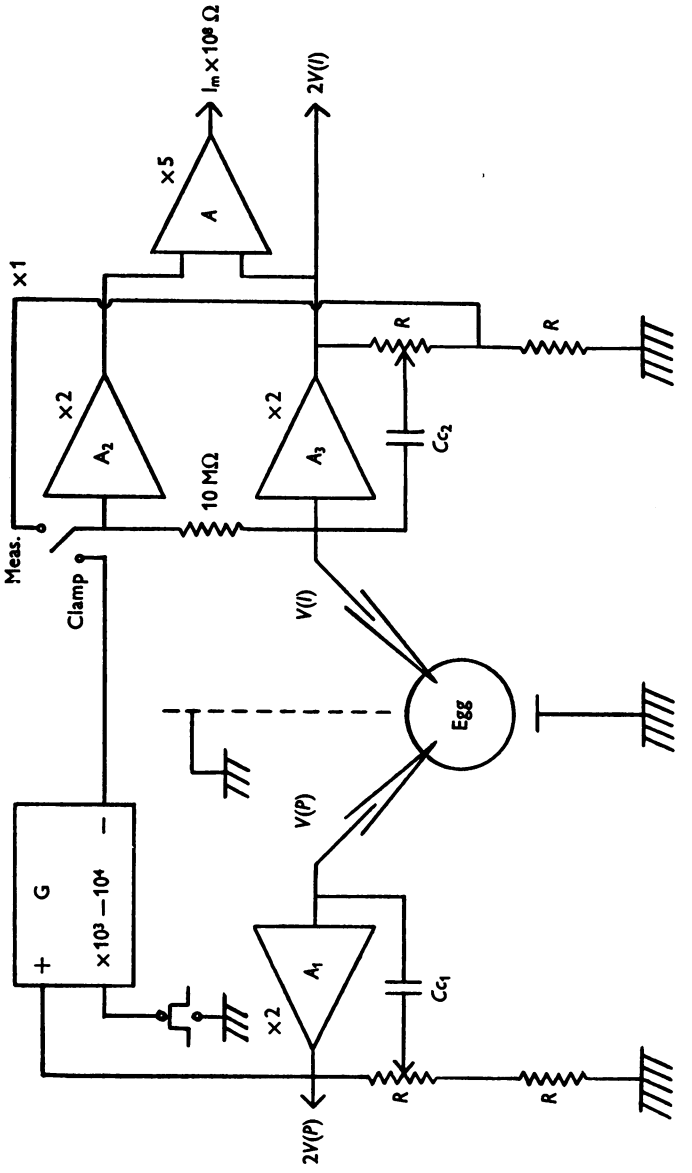

Fig. 1. The block diagram of the voltage-clamp circuit. A_1, A_2, A_3; FET input preamplifiers. G, high gain d.c. amplifier. $V(P)$: voltage at the micro-electrode for potential recording. $V(I)$: voltage at the micro-electrode for current injection. The membrane current (I_m) was recorded as the voltage drop of $I_m \times 10^8\ \Omega$.

The voltage clamp upon the egg cell membrane was performed as follows: Two micropipettes filled with 3M-KCl were introduced into the egg, one being for potential recording and the other for current injection. The electrode resistances used were between 8 and 15 MΩ. For current injection we specially selected the ones with resistance less than 10 MΩ. Since the egg surface was fairly spherical and the potential and current electrodes were introduced into the cell with a mutual angle of 60° at the centre of the egg (Eisenberg & Engel, 1970), the membrane of the egg (270 μm in diameter) was considered to be under the space clamp condition. (Actually potential responses obtained from the two electrodes coincided exactly with each other, when constant current stimulation was applied through either electrode.) A block diagram of the voltage-clamp circuit is illustrated in Fig. 1. Principles of the circuit were essentially the same as those of previous investigators (Hodgkin, Huxley & Katz, 1952; Moore & Cole, 1963). Some features of this circuit to be noted are as follows: (1) Membrane currents were measured by the voltage drop across a 10 MΩ resistor inserted between the current micro-electrode and the output of the feed-back amplifier (G). (2) Besides the potential electrode, the current electrode as well could record the potential change if the switch position was at Meas. This was especially useful to adjust the critical electrode position to stabilize the penetration. (3) Besides Cc_1 for the recording electrode, Cc_2 was attached to compensate the stray capacity of the current electrode against the ground, and to improve the high frequency response of the clamped potential. (4) The feed-back amplifier (G) consisted of two blocks of operational amplifier circuits in series, each of which had a negative feed-back loop and the equalized frequency responses up to 10 kHz.

The capacitative transient of the egg membrane currents (total membrane capacity 2×10^{-9} F; see Miyazaki *et al.* 1974*a*) with this clamp circuit usually terminated within a millisecond as illustrated in Fig. 2*A*. The potential error or the deviation from the exact rectangular step due to the large membrane current ($1{\cdot}85 \times 10^{-8}$ A in case of Fig. 2*B*) was less than 1·5 mV/10^{-8} A as shown in Fig. 2*B* (ΔV_e), the error being proportional to the amount of the current. Thus, neglecting this error, the potential measurement was done at the final steady level (upward arrow). In the usual experimental procedure, the command voltage pulse was applied every 11 sec and the current record was first memorized in a 8 bits 1K words transient recorder (Kawasaki Electronica TM 1510) with various clock rates of 0·02–0·5 msec and was then illustrated on the graphic paper by a high speed, balanced type, d.c. pen recorder (Rikadenki B-26 MARK II) during the resting interval between the successive command pulses.

RESULTS

Transient inward membrane currents of the tunicate egg in standard artificial sea water. As previously described, the egg cell membrane showed a low resting potential of 5 to −10 mV and the characteristic 'off response' was evoked after the large hyperpolarization beyond −70 mV, its critical membrane potential being about −45 mV (Miyazaki *et al.* 1974*a*).

When the voltage clamp of the egg membrane was performed, the membrane potential was first held at −90 mV to avoid the inactivation of the inward currents. Eggs in which the holding currents were hyperpolarizing currents of less than 5×10^{-10} A, were selected for the experiments. If the holding current exceeded that value, the membrane showed poor inward current and less marked non-linearity in the steady-state

V-I relation. The non-linearity or the inward-going rectification was characteristic for the egg membrane and was precisely described in the previous papers (Miyazaki *et al.* 1974*a*; Miyazaki, Takahashi, Tsuda & Yoshii, 1974*b*).

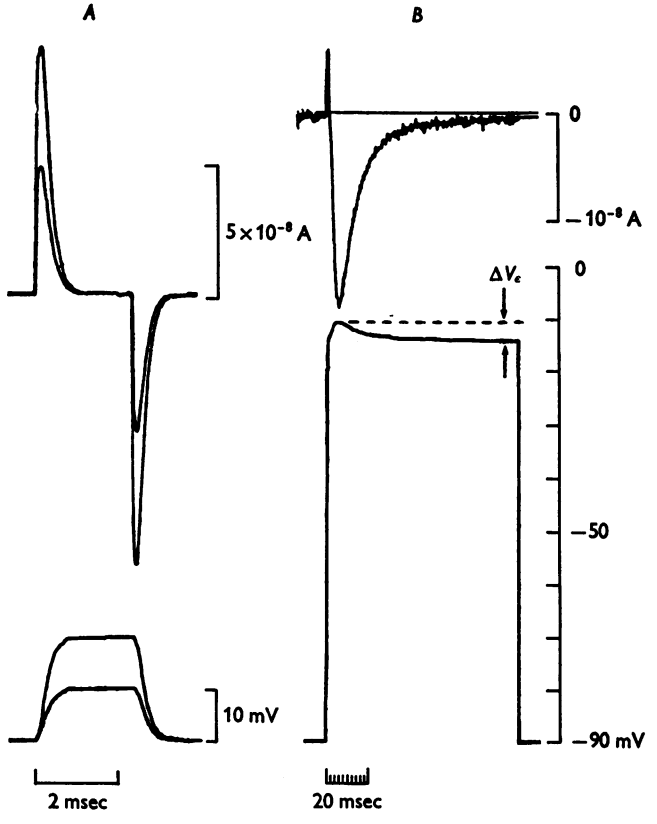

Fig. 2. *A*: the capacitative currents during the voltage steps illustrated in upper traces. *B*: the demonstration of the potential error (ΔV_c) from the rectangular step due to the large membrane current. Lower trace: the membrane potential. Upper trace: the corresponding membrane current. At the peak of the current of $1{\cdot}85\times10^{-8}$ A, the potential error was able to be reduced within 1·5 mV/10^{-8} A. Egg: EVC-34.

The voltage steps were applied upon the holding level and the corresponding membrane currents were illustrated in Fig. 3*A*. The figure on the left side of each trace indicates a membrane potential level attained by the respective voltage step. As expected from the critical membrane potential of the 'off response', the inward current began to flow with the depolarization beyond −52·5 mV, and its maximum current was observed around −30 to −25 mV, the amount ranging from 1 to 3×10^{-8} A at 15° C.

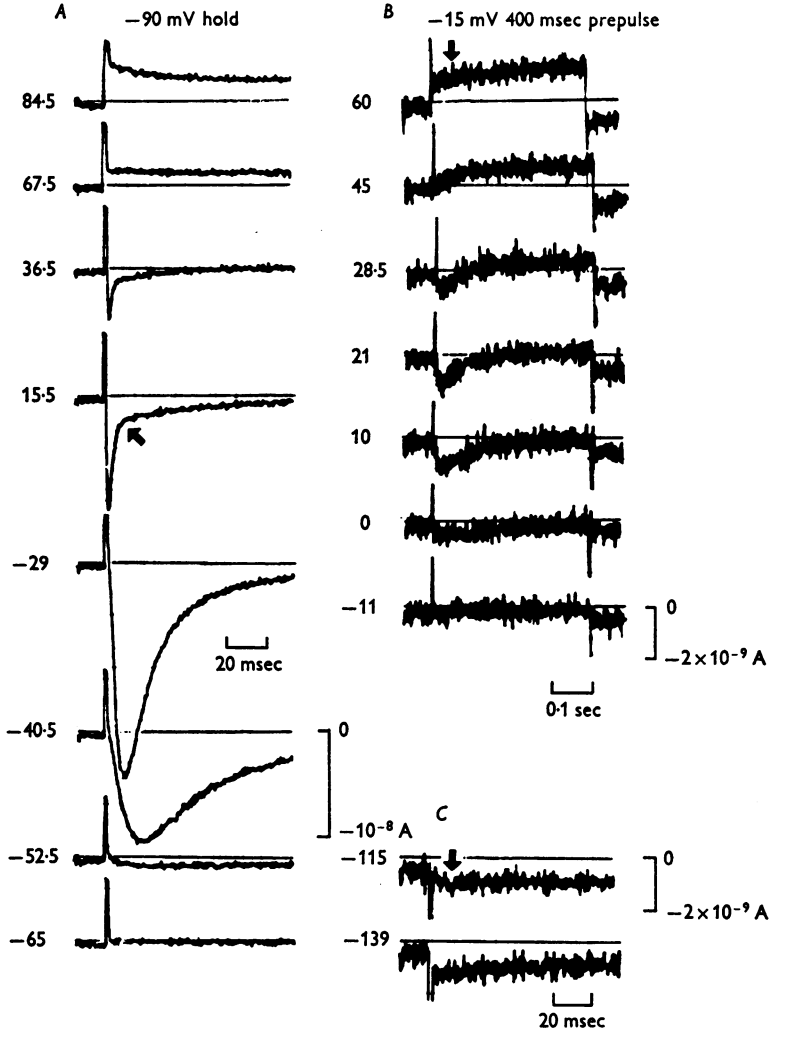

Fig. 3. The membrane currents under step changes of controlled membrane potential in standard artificial sea water (standard ASW) at temperature 14° C. Egg: EVC-9. *A*: membrane currents in response to single voltage step. The holding potential was −90 mV in this and succeeding Figures unless otherwise noted. The holding current was $-4{\cdot}5 \times 10^{-10}$ A (hyperpolarizing current) in this egg. The figures on the left side of current traces indicate the membrane potential in mV. The arrow on the trace of 15·5 mV indicates the appearance of slower component of the inward current which was superposed upon the falling phase of the major and faster component. *B* illustrates the minor component in isolation from the major component by inactivating the major one completely with the conditioning depolarization at a potential level of −15 mV lasting 400 msec. The figures on the left side of traces indicate potential levels finally depolarized by test pulses. Arrow shows possible delay for the activation of outward rectifying conductance. *C* illustrates membrane currents in response to the hyperpolarizing potential steps from −90 to −115 and −139 mV respectively. The arrow shows existence of delay in the activation of the inward current induced by anomalous rectification.

The characteristic features of the membrane currents for the voltage steps in the egg were as follows. (1) The membrane currents were transient and mostly directed inwardly in the range of the membrane potential up to +60 mV. Above that level the whole currents became outward. (2) The outward current appeared first around 20 mV at the end of the voltage pulse or at the steady state of the current, though the amount was extremely small. Above 60 mV there was a sign of K activation which is known to appear in the squid axon at a far more negative potential level (Hodgkin & Huxley, 1952*b*). (3) The transient inward current revealed both activation and inactivation as in the case of the Na inward current of other excitable membranes (Hodgkin & Huxley, 1952*b*, *c*, *d*; Hodgkin, 1958). (4) The time courses of the activation and inactivation were membrane potential-dependent. The more positive an inside potential was, the faster both time courses became, these being common to the usual Na inward current (Hodgkin & Huxley, 1952*b*, *d*). In spite of the relatively slow changes in the egg action potential (order of seconds) observed in the potential responses to the constant current stimulation (Miyazaki *et al.* 1974*a*), the time courses of the inward current under the voltage-clamp condition were rather fast. For example, time to the peak of the maximum inward current at −29 mV in Fig. 3*A* was 10 msec at 15° C, which was roughly 20 times larger than that of Na inward current of the myelinated fibre of the amphibian at the same potential level and at the same temperature considering that the Q_{10} of the time course of the Na current is about 3 (Dodge & Frankenhaeuser, 1958, 1959; Frankenhaeuser, 1960; Hille, 1967). (5) The time course of the falling phase or the inactivation of the inward current was exponential, as will be described later. However, with a larger voltage step beyond 0 mV, the falling phase evidently included another component of the inward current which was less in amount and had slower time course than the major component of the currents activated at −52·5 mV (arrow on the trace of +15·5 mV). In Fig. 4*A*, amounts of the current at the peak of the transient phase (filled circles) and the steady state (filled triangles) were plotted against the membrane potential. Since the steady component of the currents was extremely small in comparison with the transient one, no correction of so called 'leakage current' was made in Fig. 4*A*. Furthermore, since the steady state *V-I* relation in the tunicate egg was markedly non-linear as described previously, it was difficult to subtract the 'leakage current' assuming the linearity of the current. The initiation of the transient inward current was first observed at −52·5 mV, and the current became half of its maximum peak ($2{\cdot}1 \times 10^{-8}$ A) at −40·5 mV ($E_{I_p} = \frac{1}{2} I_{p.max}$; the horizontal interrupted line and arrow). As the outward current was evident above 60 mV, the reversal potential of the transient inward current was

estimated by the potential at which the *V-I* curve at the peak of the transient inward current crossed that of steady outward one. In case of Fig. 4*A*, this was equal to +67·5 mV (downward arrow). The *V-I* relation was quite similar to that of the separated Na current of the squid giant

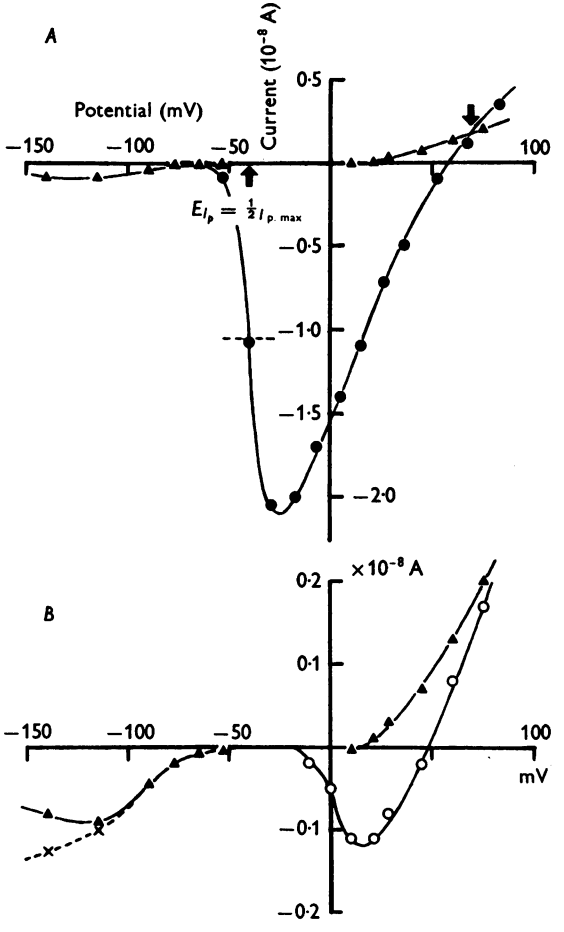

Fig. 4. The same unfertilized egg as illustrated in Fig. 3. Egg: EVC-9. *A*: the *V-I* relations at the peak of the transient membrane current (filled circles) and at the steady level of the current (filled triangles) under the voltage-clamp condition. Horizontal interrupted line indicates a half amount of the maximum peak inward current. The corresponding membrane potential is represented as $E_{I_p} = \frac{1}{2} I_{p.max}$. Downward arrow: reversal potential. *B* illustrates the *V-I* relations of the same steady current as in Fig. *A* with an expanded current scale (filled triangle) and of the minor component of the inward current isolated with conditioning prepulse to −15 mV (open circle). *X* indicates an initial transient current with a hyperpolarizing potential pulse.

axons or myelinated fibres (Hodgkin *et al.* 1952; Hodgkin & Huxley, 1952*a*, *b*; Dodge & Frankenhaeuser, 1959; Hille, 1967).

Major and minor components of the transient inward current. On the removal of Na ion in the external solution either by replacing with Tris or choline ion, most of the inward currents in std ASW disappeared as shown in Fig. 5*A*, 10 Ca, Na-free choline ASW. With close inspection,

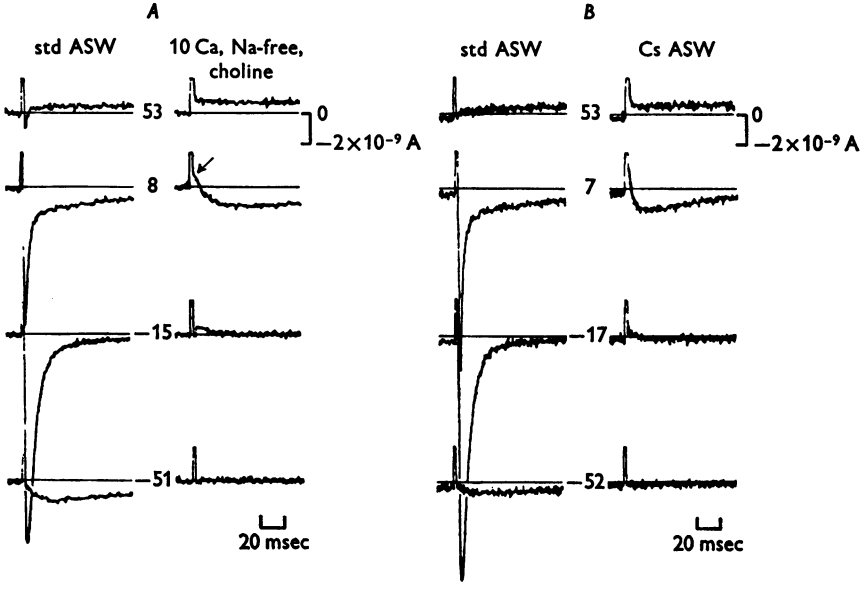

Fig. 5. *A*: the effect of Na removal from the external solution upon the transient inward currents under the voltage-clamp condition. The egg: EVC-2. 12° C. Left traces were obtained in standard (std) ASW while right traces were obtained in choline ASW without Na. Each set of the left and right traces was observed at the same potential level as indicated in mV in the middle of two traces in this Fig. 5*A* and the next Fig. 5*B*. The arrow indicates the reversed major component of the transient inward currents. B: the effects of the replacement of Na in standard ASW with Cs upon the major component of the inward current. The egg: EVC-38. 14·5° C. Left traces were obtained in standard ASW while right traces were obtained in Cs ASW.

besides the abolition of the inward currents a reversed transient outward current was observed as in case of the trace of −15 mV in 10 Ca, Na-free choline ASW. At +8 mV level, the fast or major component of the inward current was clearly reversed to an outward current (arrow), but the slow or minor component which had been seen on the falling phase of the major component in standard ASW remained unchanged in its polarity and in its amount even after the removal of Na.

It was concluded that the major component was Na current and the reversed outward transient current was probably the outward flux of Na ions in the absence of external Na. In Fig. 6*A* and *B*, peak values of inward and outward Na transient currents were plotted against membrane

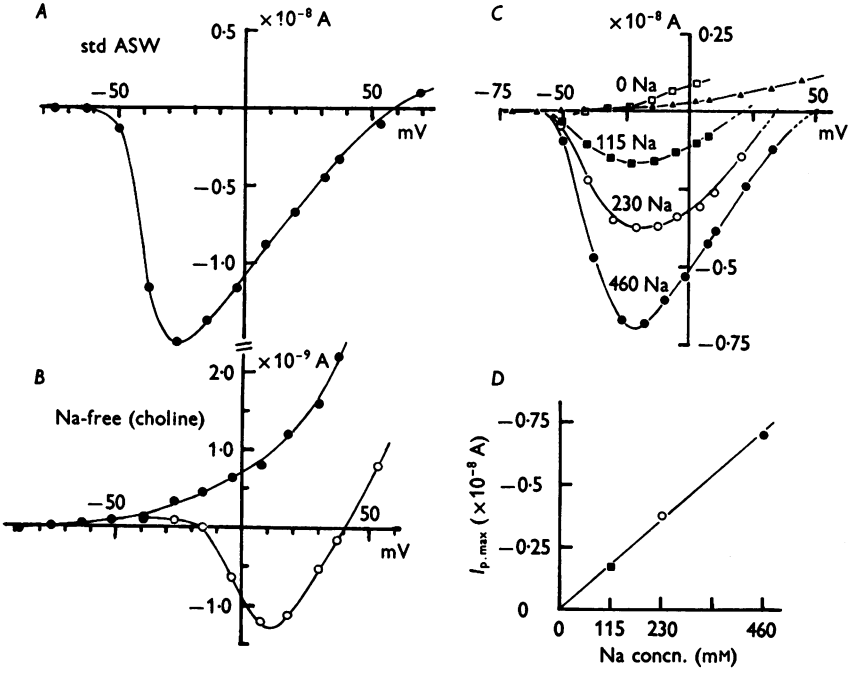

Fig. 6 The *V-I* relations at the peak of the transient membrane currents in standard ASW (*A*) and in Na-free choline ASW (*B*). The same unfertilized egg as illustrated in Fig. 5*A*: EVC-2. Filled circles (●) indicate the major component of the inward currents in standard ASW and its reversed outward transient membrane current in Na-free choline ASW. Open circles (○) indicate the minor components of the inward currents which remained unchanged in Na-free ASW. *C*: a series of *V-I* relations at the peak of the major or Na component of the inward current in the ASW of various Na concentration indicated in mM by the figures on each *V-I* curve. From an unfertilized egg; HVC-33. Temperature 8–9° C. *D*: plotting the maximum of the peak, Na inward current ($I_{p.max}$) at −25 mV against Na concentration in ASW. The same unfertilized egg illustrated in Fig. *C*. Filled triangles in *C* indicate the steady-state currents in standard ASW.

potential in standard ASW and 10 Ca, Na-free choline ASW respectively, and the remaining minor component was also plotted with open circles (Fig. 6*B*). The critical membrane potential and the time courses of the activation and the inactivation seem to be common between inward and outward Na currents. All these characteristics of Na current are the same

as those which have been observed in Na current of the squid axon or myelinated fibres (Hodgkin & Huxley, 1952*a*, *b*; Dodge & Frankenhaeuser, 1958, 1959; Frankenhaeuser, 1960).

The partial replacement of Na ions in the external solution resulted in the reduction of the peak amplitude of the inward current and of the reversal potential, while the critical membrane potential and the potential level at which the inward current became maximum remained at the same level as in standard ASW. The *V-I* relations in ASWs with various amounts of Na concentration were shown in Fig. 6*C* and the peak I_{Na} of the maximum inward current was plotted against Na concentrations in Fig. 6*D*. The results showed a linear relation between the maximum current and Na concentration. These can be expected from the independence principle which has been proved to be valid for the Na inward current of squid giant axons (Hodgkin & Katz, 1949; Hodgkin & Huxley, 1952*a*).

From the experiment in 10 Ca, Na-free choline ASW, the minor component of the inward current was found to be activated around -10 mV (Fig. 6*B*), the critical level being far more positive than that of the major component or Na current. When we applied 400 msec duration prepulse to -15 mV preceding the test pulse in standard ASW, the major component of the transient inward current evoked by the test voltage step was completely abolished, while the minor and slower component of the inward currents still remained (Fig. 3*B*). The minor component which remained after such an inactivation of the major component had a critical membrane potential of about -10 mV again corresponding to the value obtained in the choline ASW. The minor component showed also the process of activation and inactivation. The maximum peak current $1{\cdot}1 \times 10^{-9}$ A was obtained around $+15$ mV (Fig. 4*B*, open circle) and the peak time of the maximum current was 20 msec. It was noticed that the shape of *V-I* relation at the peak of the minor component isolated with prepulse in standard ASW was exactly the same as that obtained in Na-free choline ASW (Fig. 6*B*). The peak current of the minor component was about one twentieth of that of the major one and its level of activation was at least 40 mV more positive than that of the major one.

It had already been described that Na and Ca action potentials existed in *Halocynthia* eggs, and the critical membrane potentials for Na and Ca currents were about -45 and 0 mV respectively at the standard Ca concentration of 10·6 mM (Miyazaki *et al.* 1974*a*). As already mentioned in the early part of this section, the major component was identified as Na current and the succeeding paper will show that the minor component exactly corresponds to Ca current. The later description of the present paper will mainly concern the major component or Na current. Collected

data of the parameters of the major and minor components are illustrated in Table 2*A* and *B*.

Effects of replacement of Na in standard ASW with Li or other alkaline cations and of addition of tetrodotoxin 5×10^{-6} *g/ml. to the external solution.* As shown in Fig. 7*B*, the replacement of external Na with Li ions did

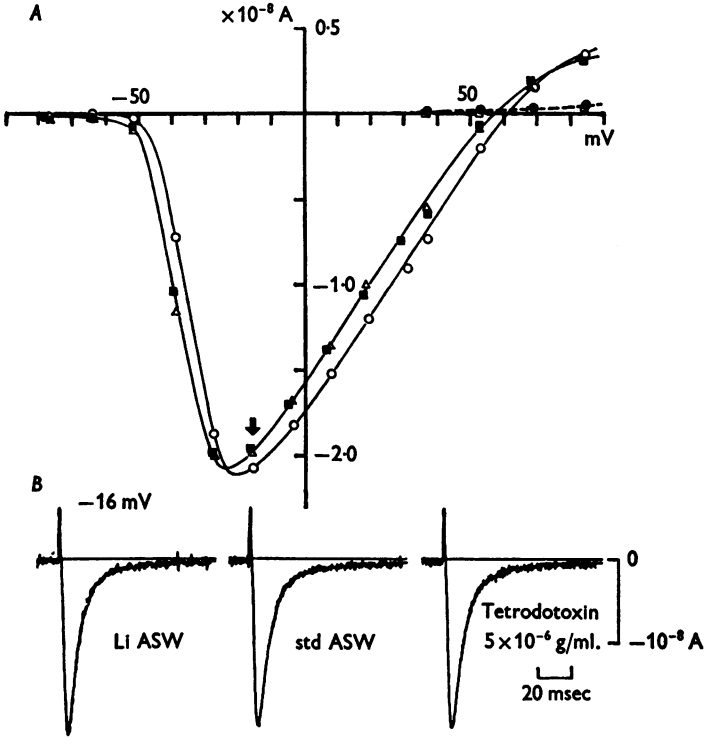

Fig. 7. The effects of the replacement of Na in ASW with the same molar concentration of Li and of the addition of tetrodotoxin 5×10^{-6} g/ml. to standard ASW upon the major component of the inward current at −16 mV (*B*: see arrow in *A*) and their *V-I* relations at the peak of the inward current (continuous line) and at the steady state (interrupted line) (*A*). ■ □: standard ASW, △; standard ASW with tetrodotoxin 5×10^{-6} g/ml., ○, ●: Li ASW. Egg: EVC-34. Temp. 12·5° C.

not change the transient inward current significantly. This would be expected from the fact that Li can always be substituted for Na in the transient inward current of other excitable membranes (Overton, 1902; Hodgkin & Katz, 1949; Chandler & Meves, 1965; Moore, Anderson, Blaustein, Takata, Lettvin, Pickard, Bernstein & Pooler, 1966; Hille, 1972).

TABLE 2*A*, characteristics of the major (Na) component of transient inward current in the egg cell membrane

Egg number	Temp. (°C)	ASW	Holding* current ($\times 10^{-10}$ A)	c.m.p.† (mV)	$E_{I_{p.max}}$ (mV)	$I_{p.max}$‡ ($\times 10^{-9}$ A)	$E_{Ip} = \frac{1}{2}I_{p.max}$§ (mV)	Time course of the maximum inward current: Half-rise‖ time (peak time) (msec)	Time course of the maximum inward current: Half-decay‖ time (msec)	Reversal potential
EVC 4	15	std	−4·5	< −52·5	−28	−15·6	−42	4·0 (8·0)	9·0	—
EVC 5	15	std	−4·2	< −52·5	−28·5	−17·1	−41·5	5·0 (9·0)	11·0	—
EVC 6	14·5	std	−4·7	< −51·5	−27·5	−35·0	−45·0	5·5 (12·0)	13·5	58
EVC 7	14·2	std	−4·5	< −52·5	−28	−9·5	−42·0	4·8 (9·0)	11·0	—
EVC 8	14·2	std	−4·0	< −52·5	−28	−13·8	−41·0	4·0 (8·5)	12·0	58
EVC 9	15·0	std	−4·8	< −52·5	−29	−20·5	−40·5	5·6 (10·0)	13·6	58
EVC 10	15·5	std	−3·5	< −52·5	−29·5	−26·6	−44·0	3·5 (6·0)	8·3	—
EVC 11	15·4	std	−4·0	< −51·5	−27·5	−27·6	−46·5	3·8 (7·4)	8·6	58
EVC 29	15	std	−1·0	< −52	−28	−24·7	−43·5	3·4 (7·4)	8·6	67·5
EVC 31	14·5	std	−6·5	< −53	−31	−32·0	−46·0	3·4 (7·4)	6·2	62·5
EVC 38	14·5	std	−3·7	< −51·5	−27·5	−36·0	−40·0	3·6 (7·4)	9·9	—
EVC 41	14	std	−0·5	< −52	−27	−26·0	−43·5	2·8 (6·4)	6·8	62·5
EVC 43	14·5	std	−2·2	< −51·5	−27·5	−28·3	−43·0	2·8 (5·4)	6·0	65
EVC 44	14·3	std	−1·5	< −51·5	−27·5	−27·5	−44·5	3·0 (6·6)	6·8	—
EVC 45	14·5	std	−3·8	< −51·5	−26·5	−22·6	−39·5	3·0 (6·4)	7·6	68
EVC 46	16·5	std	−2·0	< −51·5	−27	−20·0	−39·5	3·0 (6·4)	6·8	68
EVC 47	16	std	−6·0	< −51·5	−27	−33·0	−39·0	3·0 (5·0)	5·4	62
EVC 48	14·5	std	−1·8	< −51·5	−27	−24·0	−42·5	3·3 (6·5)	7·0	
EVC 50	14·1	std	−4·2	< −52	−28·5	−48·0	−43·5	3·6 (7·0)	6·2	59
EVC 51	14·5	std	−2·8	< −51	−27	−26·1	−39·0	3·6 (7·0)	6·2	60
EVC 52	14·5	std	−1·3	< −51	−27	−13·6	−41·5	4·0 (8·0)	8·6	67
Average and S.D.			−3·4 ± 1·6		−27·8 ± 1·0	−25·1 ± 8·7	−42·3 ± 2·2	3·7 ± 0·8 (7·5 ± 1·6)	8·5 ± 2·4	62·4 ± 3·9

* Holding potential −90 mV.
† Critical membrane potential.
‡ The peak of the maximum inward current.
§ The potential level at which the peak I_{Na} becomes a half of that of $I_{Na.max}$
‖ Δt

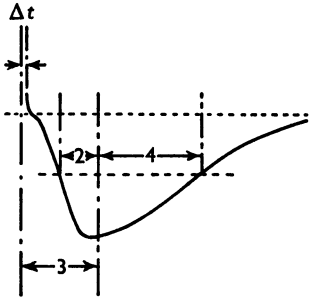

1, Δt delay time (see text p. 624);
2, half-rise time;
3, peak time (including the delay time (1));
4, half-decay time.

B, characteristics of the minor (Ca) component of transient inward currents in the egg cell membrane

Egg number	Temp. (°C)	ASW	Holding* current ($\times 10^{-10}$ A)	Conditioning† prepulse (mV)	c.m.p.‡ (mV)	$E_{I_{p.max}}$ (mV)	$I_{p.max}$§ ($\times 10^{-9}$ A)	Peat time‖ (msec)	$\frac{I_{p.max.Ca}}{I_{p.max.Na}}$
EVC 6	14·5	std	−5·0	−20·5	< −10·0	12·5	−1·2	20	0·034
EVC 8	14·2	std	−4·0	−13·5	< −8·0	13·5	−1·0	20	0·073
EVC 9	15·0	std	−4·8	−15·0	< −11·0	10 (~20)	−1·1	20	0·049
EVC 10	15·5	std	−3·5	−15·0	< −10·0	12	−1·32	22	0·045
EVC 17	14·5	std	−2·2	−27·0	< −10·0	12·5	−1·4	18	0·145
EVC 48	14·5	std	−1·8	−39·0	< −10·0	12·5	−1·7	17	0·071
Average and S.D.						12·2 ± 1·1	−1·3 ± 0·2	19·5 ± 1·6	

* Holding potential −90 mV.
† Prepulse duration 400 msec.
‡ Critical membrane potential.
§ The peak of the maximum inward current.
‖ including the delay time due to the limitation of the high frequency response in the voltage clamp (see ‖ of Table 2*A* and text p. 624).

The *V-I* relation at the peak of the major component in Li ASW was almost similar to that in standard or Na ASW (Fig. 7*A*). However, a small positive shift of the critical membrane potential and a possible shift of the reversal potential were noticed. Other alkaline cations Cs, Rb and K were also used to replace Na in ASW. In Cs ASW, the major component was mostly reversed in its polarity (Fig. 5*B*) as in Na-free choline ASW, though a residual inward current was seen at about -40 mV, indicating a slight permeability to Cs. In K and Rb ASW, small transient inward currents were visible around the potential range where the major component was dominant (not shown with a figure), besides the steady inward currents of K and Rb flowing through the inward rectifying conductance of the egg membrane (Miyazaki *et al.* 1974*a*; Miyazaki *et al.* 1974*b*). The permeability sequence of the egg Na channel had the order of Li > Na > K > Rb > Cs. The preliminary estimation of the permeability ratio of the egg Na channel among alkaline cations was obtained from the apparent shifts of the reversal potential of the major component in various ASWs from that in standard or Na ASW. The obtained values 1:0·088:0·045:0·027 for Na:K:Rb:Cs coincided well with those of the squid axons or the myelinated fibre (Chandler & Meves, 1965; Moore *et al.* 1966; Frankenhaeuser & Moore, 1963*b*; Hille, 1972).

The specific Na channel inhibitor, tetrodotoxin (Narahashi, Moore & Scott, 1964; Nakamura, Nakajima & Grundfest, 1965; Moore, Blaustein, Anderson & Narahashi, 1967; Rojas & Atwater, 1967), had no effect on this Na inward current of the tunicate egg even in a large amount of 5×10^{-6} g/ml. The *V-I* relations at the peak of Na current were exactly identical in the presence of tetrodotoxin.

Nature of the inactivation of Na channels in the egg cell membrane. The inactivation of Na current of the egg was studied by observing the reduction of the maximum inward current with various prepulses of 400 msec at temperature 14° C, the conditioning level being ranged from -150 to -30 mV. Fig. 8*A* illustrates such a series of the inward currents. The conditioning depolarization above -90 mV reduced the amplitude of the inward current, but neither the peak time nor the half-decay time of the current was significantly changed. In other words, the time course of the current remained almost unchanged while the amplitude altered separately.

The peak amplitude of the membrane current, as a relative value, was plotted against the potential level of the conditioning pulse in three experiments (Fig. 8*B*). The inactivation curve was S-shaped. Similar S-shaped curves have been observed for Na channels in other excitable membranes (Hodgkin & Huxley, 1952*c*; Frankenhaeuser, 1959, 1960). Assuming no inactivation at a potential level of -150 mV, i.e. $V_{h=1\cdot0} =$

-150 mV, $V_{h=\frac{1}{2}}$ was equal to -56 mV. The e-fold changes of $h/(1-h)$ value were obtained by 5·8 mV increase in the membrane potential in the portion of the curve above $-67{\cdot}5$ mV (real line in Fig. 8*B*). Thus, inactivation curve could be approximated as following equations: $1/[1+\exp\{(V-V_h)/K_h\}]$; $V_h = -56$ mV, $K_h = 5{\cdot}8$ mV, $V > -67{\cdot}5$ mV, where V indicates a potential level of the conditioning prepulse. The V_h and K_h

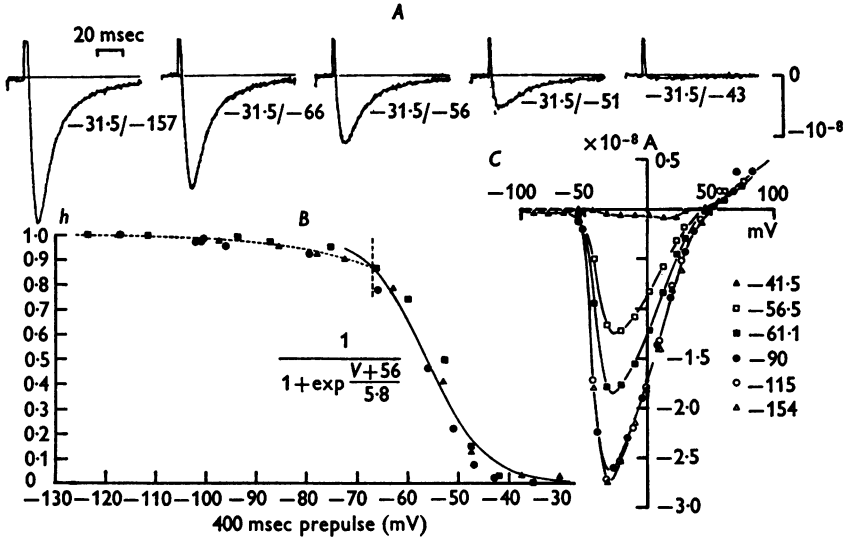

Fig. 8. Inactivation of Na inward current by the conditioning depolarization. Temperature 13–14° C. *A* shows a series of Na currents with a definite test potential level of $-31{\cdot}5$ mV preceded by various conditioning depolarization of 400 msec duration indicated in mV by the denominator of the fractional numbers on the respective current traces. Egg: EVC-11. *B* shows an inactivation curve of Na currents from three unfertilized eggs including the one illustrated in *A*. Eggs: EVC-11 (●), EVC-44 (■) and EVC-45 (▲). Test pulse levels were $-31{\cdot}5$, -20 and -20 mV for ●, ■ and ▲ respectively. *C* shows a series of *V-I* relations at the peak of Na currents obtained by changing test potential pulses preceded by six definite levels of the conditioning depolarization, being indicated in mV by figures in the inset.

values of the egg membrane were approximately the same as those of the axonal membranes, such as squid axons (Hodgkin & Huxley, 1952*c*; Chandler, Hodgkin & Meves, 1965, where $V_h = -59$ mV, $K_h = 7{\cdot}0$ mV) or myelinated fibres (Frankenhaeuser, 1959, where V_h = resting potential (probably -70 mV) + 9·15 mV, $K_h = 8{\cdot}17$ mV). Below $-67{\cdot}5$ mV e-fold changes of $h/(1-h)$ value required 15·0 mV increase in the membrane potential (the interrupted line in Fig. 8*B*). There was a deviation of the relation between $h/(1-h)$ and the membrane potential from a single exponential function.

With conditioning depolarization longer than 400 msec, the inactivation curve slightly shifted to the negative potential side. For example with 3 sec prepulse, V_h became -68 mV. The long lasting depolarization seemed to induce a slow inactivation of Na current to a slight extent. The apparent slow inactivation of Na channels has been found in NaF-perfused squid axons (Chandler & Meves, 1970) and in scorpion toxin-exposed myelinated fibres (Koppenhöfer & Schmidt, 1968). The deviation of the $h(400\text{ msec})/\{1-h(400\text{ msec})\}$ function from a single exponential one may be related to this slow inactivation. The precise analysis of the inactivation process of Na channels in the egg cell membrane is now in progress.

When Na inward current was partially inhibited by the conditioning depolarization, the time course of the current increase was almost unchanged. Further, in Fig. 8*C*, six *V-I* curves at the peaks of the inward currents were plotted against potential levels of the test pulses preceded by six different conditioning levels which were indicated in insets of the Figure. The obtained *V-I* curves resembled each other in their shape and were different only in their relative amplitude. The above two results suggested that the activation process was independent of the inactivation process also in this egg membrane, as expected from the Hodgkin–Huxley model (Hodgkin & Huxley 1952*d*).

In Fig. 9*A*, the time course of Na current with a test pulse to -15 mV was plotted in the semilogarithmic scale. As shown by vertical arrows, the tail of the falling phase deviated from a single exponential decay. The deviation could be observed even at the potential where Na inward current was dominant while Ca current was not yet activated. This corresponds to the slow inactivation of Na current above mentioned. Admitting the existence of this inactivation, the time course of the falling phase of the current as well as the inactivation curve would be slightly changed with the variation of the duration of the conditioning prepulse. In the following analysis, however, the effect of the slow inactivation will be neglected for a first order approximation.

Kinetic parameters of egg Na current. Since the activation process was confirmed to be independent of the inactivation process, the Na inward current can be formalized in terms of m and h parameters as follows:

$$i = m^n h \bar{I}_{Na}.$$

Here,

$$m = m_0 + (m_\infty - m_0)(1 - e^{-t/\tau_m}),$$

$$h = h_\infty + (h_0 - h_\infty)e^{-t/\tau_h},$$

$$\bar{I}_{Na} = \bar{g}_{Na}(E_m - E_{Na}),$$

$E_m - E_{Na}$, driving force for Na. Other parameters; the same meanings as in squid axons (Hodgkin & Huxley, 1952*d*).

Since at the holding level of -90 mV there was no trace of the transient inward current, m could be described as $m_\infty(1-e^{-t/\tau_m})$. From Fig. 8*B*, at the potential above -40 mV, h_∞ will be almost zero. Thus if the time t is very much less than τ_m, i is nearly equal to $\bar{I}_{Na}.h_0.m_\infty^n(t/\tau_m)^n$. The

log-log plotting of the initial portion of the inward current against the time t suggested that n was nearly equal to 2. Therefore, in order to describe the inward current, the equation: $i = \{m_\infty(1-e^{-t/\tau_m})\}^2 h_0 e^{-t/\tau_h} \bar{I}_{Na}$ will be suitable. In Fig. 9*A*, an example of Na inward current at a potential level of $-15{\cdot}0$ mV and at 13·5° C, illustrated in the inset of Fig. 9*B*, was analysed by plotting against the time from the initiation of the command pulse in the semilogarithmic scale.

For the analysis of the initial portion of the inward current, the increased clock rate of the memory, interval 0·02–0·05 msec, was used whenever necessary.

The plotted i_{Na} was the value obtained, in case of Fig. 9, by subtracting the small steady current from the total inward current, although the absolute value of the steady current in standard ASW was less than 2×10^{-10} A in the potential range from -50 to $+20$ mV and negligible in most cases.

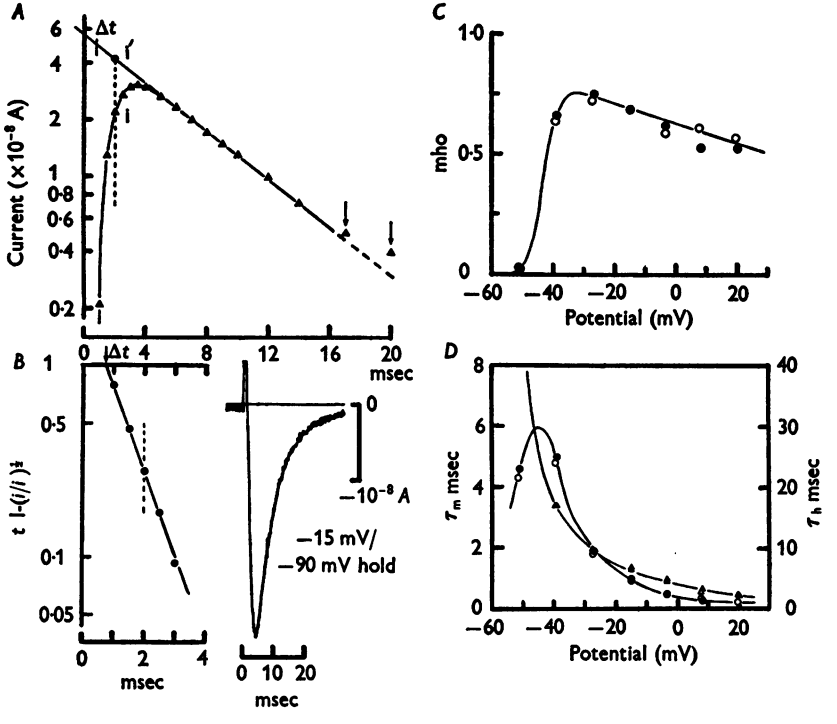

Fig. 9. Analysis of the time course of Na inward current. *A* and *B* illustrate the methods of determining kinetic parameters of τ_m and τ_h from an example of the inward current shown in the inset of *B*, which was evoked by a potential step to -15 mV at temperature 13·5° C. For the meanings of i, i' and Δt, see the text. *C* and *D* show potential dependency of $\bar{g}_{Na} m_\infty^2$, τ_m and τ_h respectively. Two series of experiments were plotted together with filled and open symbols. In Fig. 9*D*, ●, ○ indicate τ_m and ▲, △ indicate τ_h. Temperature 13·5° C in *C* and *D*. The egg in *A*, *B*, *C* and *D*: EVC-6.

The falling phase is exactly on a straight line except at the tail or the portion below $0{\cdot}5 \times 10^{-8}$ A. The tail deviated usually upward from a single exponential decay (vertical arrows; see the footnote in the previous paragraph). It should be noted that the minor component of the inward currents had not been activated yet at this level of potential. The straight line can be represented by the equation $i' = \bar{I}_{Na} m_\infty^2 h_0 \, e^{-t/\tau_h}$ and $\tau_h =$ 6·8 msec can be obtained from its slope. We assumed that the h_0 at the holding level of -90 mV was nearly equal to 1. The square root of the ratio of i to i', $(i/i')^{\frac{1}{2}}$, should be equal to the value: $(1-e^{-t/\tau_m})$. Thus, if $\{1-(i/i')^{\frac{1}{2}}\}$ were plotted against the time in the semilogarithmic scale, we could obtain a straight line, of which the slope gave us $\tau_m = 1{\cdot}0$ msec (Fig. 9*B*). However, it should be noted that the straight line did not cross the portion of $1-(i/i')^{\frac{1}{2}} = 1$ or $i = 0$ at the time zero, but did it at the time of $\Delta t = 0{\cdot}75$ msec after the initiation of the command pulse. The delay time Δt probably corresponded to the delay of the membrane potential response due to the large surge of the membrane capacitative current, as shown in Fig. 2*A*. Thus, assuming that the voltage step apparently initiated at time Δt, it was found to be reasonable to describe the membrane current i as $\bar{I}_{Na} m_\infty^2 (1-e^{-t'/\tau_m})^2 e^{-t'/\tau_h}$ by replacing t with $t' = t - \Delta t$. The driving force for egg Na channel $(E_m - E_{Na})$ was calculated as -73 mV from the reversal potential of the major component (58 mV in this case) for the inward current of the inset of Fig. 9*B*. Thus, $\bar{g}_{Na} m_\infty^2$ was 0·685 μmho.

The obtained conductances $(\bar{g}_{Na} m_\infty^2)$ and time constants (τ_m, τ_h) were plotted against the membrane potential in Fig. 9*C* and *D* respectively. The relation between the $\bar{g}_{Na} m_\infty^2$ and the membrane potential showed a maximum at about -35 mV in Fig. 9*C*. It may be reasonable to consider that m_∞ became saturated approximately at -30 mV and $\bar{g}_{Na}$ decreased gradually with the more positive membrane potential rather than that m revealed the maximum at -35 mV. The decrease in $\bar{g}_{Na}$ can be explained by assuming that Na conductance had a constant field type rectification as in case of myelinated axons (Frankenhaeuser, 1960). τ_m seemed to attain its maximum between -50 and -40 mV. τ_h became extremely large at -50 mV (more than 100 msec). The supposed maxima of τ_m and τ_h almost corresponded with those of squid axons and myelinated fibres (Hodgkin & Huxley, 1952*d*; Cole, 1968; Frankenhaeuser, 1960; Hille, 1971). The collected data of τ_m and τ_h of the major component in standard ASW are listed in Table 3.

In 10 Mn ASW where Mn^{2+} ions substituted for Ca^{2+} in standard ASW, there was almost no minor component (Okamoto, Takahashi & Yoshii, 1976). Therefore, the value τ_h was successfully calculated up to the level $+30$ mV of the membrane potential. In low temperature of 3·5° C, the value τ_m could be calculated also up to

TABLE 3. The collected data of τ_m and τ_h for the major or Na component of the inward currents

			τ_m (msec) Membrane potential in mV								τ_h (msec) Membrane potential in mV							
Egg	ASW	Temp. (°C)	−51·5	−39·0	−27·5	−15·0	−4·0	7·5	19·0	30·0	−51·5	−39·0	−27·5	−15·0	−4·0	7·5	19·0	30·0
EVC6	std	13·5	4·6	5·0	1·9	0·92	0·48					17	9·6	6·5	4·5			
		9	9·9	8·9	3·5	1·54					268	30	18	12·4	8·0			
		5	24	19	7·8	4·8	2·6				336	72	38	25	15·6			
		13·5	4·3	4·8	1·8	1·0	0·49				144	17	9·8	6·8	4·8			
		18	3·7	2·5	0·92	0·62	0·35				73	9·2	6·0	3·8	2·8			
EVC-10	std*	14·5	4·4	3·6	1·7	1·05	0·65				164	21·5	10·5	6·6	4·4			
			(−53)	(−40)	(−29·5)	(−18)	(−7)				(−53)	(−40)	(−29·5)	(−18)	(−7)			
EVC-48	std	15		4·0	1·97	0·90	0·42					20·8	7·7	4·15	3·4			
		5	15·9	14·5	7·8	3·8	2·1				407	66	28·5	18·0	14·6			
		10	7·5	7·4	3·2	1·85	1·1				110	29·5	15	9·4	5·8			
		15	5·1	4·6	2·0	0·93	0·53				144	18·5	8·5	5·3	3·85			
		19	2·5	2·8	0·95	0·75	0·44				99	9·5	4·3	2·5	1·75			
EVC-36	std	12										21·5	9·7	6·0	4·6			
EVC-43	std	15									64	11·6	5·6	3·7	2·8			
EVC-40	std	13·5									131	12·6	7·3	5·2	3·6			
EVC-16	std*†	3·5	17·5	22·0	14·0	7·5	5·0	2·7	2·4	1·0	457	106·5	50·0	33·0	24·0			
			(−48)	(−38)	(−28)	(−18)	(−7)	(3)	(13)	(30)	(−48)	(−38)	(−28)	(−18)	(−7)			
EVC-48	10 Mn‡ ASW	15		6	2·56	1·21	0·78					34	13·5	7·4	4·7	3·2	2·2	1·4

* Membrane potentials which were different from those of others were presented in parentheses.

† The slowness of the time course at low temperature of 3·5° C allowed to calculate τ_m up to +30 mV.

‡ 10 mM-Ca in std ASW was completely replaced with 10 mM-Mn^{2+}. Therefore the minor component which interfered with the falling phase of the major component in the membrane potential above −10 mV was abolished.

+30 mV because of the slowness of the time course of the current. Those values are listed in Table 3 as well.

Effects of membrane potential and temperature on τ_m, τ_h *and* $\bar{g}_{Na}$. The dependence of τ_m and τ_h upon the membrane potential was further tested by plotting these parameters against the membrane potential in the semilogarithmic scale (Fig. 10*A*). The relations of both τ_m and τ_h with the

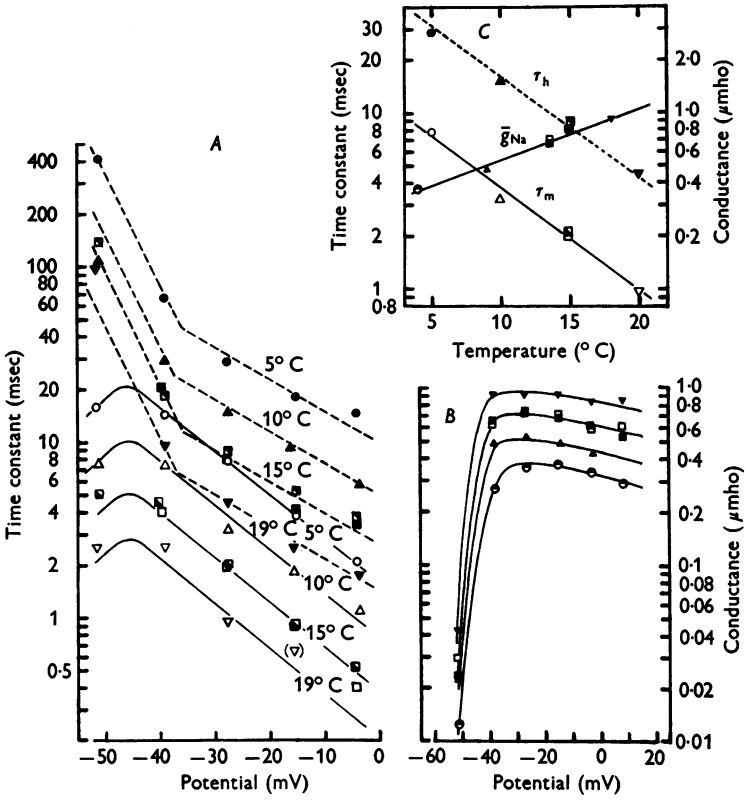

Fig. 10. The effects of membrane potential and bath temperature upon kinetic parameters of τ_m and τ_h (*A*) and chord conductance of $\bar{g}_{Na}m_\infty^2$ (*B*). *A*: plotting parameters of τ_m (open symbols) and τ_h (filled symbols) against the membrane potential with the semilogarithmic scale at four levels of the bath temperature 5·0 (○ ●), 10·0 (△ ▲), 15·0 (□ ◪, ■ ◪) and 19·0° C (▽ ▼). Symbols (◪ ◪) indicate the parameters observed on the recovery to 14·5° C after a series of changes in temperature. The egg: EVC-48. *B*: plotting chord conductance of $\bar{g}_{Na}m_\infty^2$ against the membrane potential with semilogarithmic scale at four levels of the bath temperature 4·0 (◓), 9·0 (▲), 13·5 (■ □) and 18° C (▼). Egg: EVC-6. *C*: plotting τ_ms and τ_hs at a fixed level of the membrane potential −27·5 mV against the bath temperature (from EVC-48). $\bar{g}_{Na}$s at −15 mV are also plotted against the bath temperature (from EVC-6).

membrane potential were on the straight lines in the range from -40 mV to 0 mV, suggesting approximate exponential relations. The e-fold decreases in τ_m and τ_h in Fig. 10*A* were obtained by 17 mV and 23 mV increases in the membrane potential respectively in that range. Although 17 mV for the egg τ_m may be comparable to that for τ_m of the squid axons, the increase in membrane potential required for e-fold decrease of τ_h, 23 mV, was larger than 10 mV for β_h of the inactivation of Na current of the squid membrane (Hodgkin & Huxley, 1952*d*), i.e. the τ_h of egg Na current was less sensitive to the membrane potential. However, the τ_h of egg Na current was more sensitive to the membrane potential in the range below -40 mV than above -40 mV. In the nerve membranes similarly τ_h is much more sensitive to the membrane potential in the range below -20 mV than above -20 mV (Hodgkin & Huxley, 1952*d*; Cole, 1968; Hille, 1971).

The relations of the parameters: τ_m, τ_h and $\bar{g}_{Na} m_\infty^2$, with the membrane potentials illustrated on the semilogarithmic scale did not change its shape at the various bath temperatures, as shown in Fig. 10*A* and *B*. The examined egg cell illustrated in Fig. 10*A* was first kept at the temperature 15° C and then the bath temperature was changed successively to 10, 5, 19 and 15° C. The alteration of the time courses of the inward current with the temperature change was fairly reversible, i.e., the time constants τ_m and τ_h were uniquely determined by the temperature level irrespective of previous history. Especially in case of Fig. 10*B*, the bath temperature was altered in the order of 14, 9, 4, 13·5, 18 and 13·5° C and at 14 or 13·5° C the peak currents as well were exactly the same at a fixed level of the membrane potential. The absolute values of τ_m and τ_h increased greatly by lowering the temperature, while $\bar{g}_{Na} m_\infty^2$ increased by raising the temperature. In Fig. 10*C*, τ_m and τ_h at $-27{\cdot}5$ mV and $\bar{g}_{Na} m_\infty^2$ at -15 mV were plotted against the bath temperature in the semilogarithmic scale. At this potential level, m_∞ was expected to be saturated and $\bar{g}_{Na} m_\infty^2$ equalled $\bar{g}_{Na}$. The results showed linear relations of all three parameters τ_m, τ_h, $\bar{g}_{Na}$ to the temperature in the range from 5 to 19° C. The obtained Q_{10}s for both τ_m and τ_h had exactly the same value of 4·0, while the Q_{10} for $\bar{g}_{Na}$ had a much less value of 2·0. Fig. 11*A* and *B* illustrate the relation of peak inward currents and of τ_hs at a fixed potential level around -16 mV to the bath temperature which was altered continuously from 5 to 25° C, in three eggs. The same symbols indicate the data from one egg. High Q_{10} of 4·0 for τ_h was again observed in the temperature range from 5 to 20° C, but a slightly less Q_{10} of 3·0 was obtained above 20° C. On the other hand, the Q_{10} for the peak current was 2·0 in the temperature range from 5 to 20° C, indicating that the Q_{10} for $\bar{g}_{Na}$ was much less than that for time constant τ_h. It should be noted that Q_{10} for the peak current was less than 2·0 above

20° C. In the nerve membrane, it has been reported that the Q_{10}s for τ_m and τ_h are all about 3 and the Q_{10} for $\bar{g}_{Na}$ is about 1·2 (Hodgkin *et al.* 1952; Hodgkin & Huxley, 1952*d*; Frankenhaeuser & Moore, 1963*a*, *b*; Moore, 1971; Schauf, 1973). The kinetic parameter for K conductance, τ_n, is also reported to show a large Q_{10} around 3 (Hodgkin & Huxley, 1952*d*).

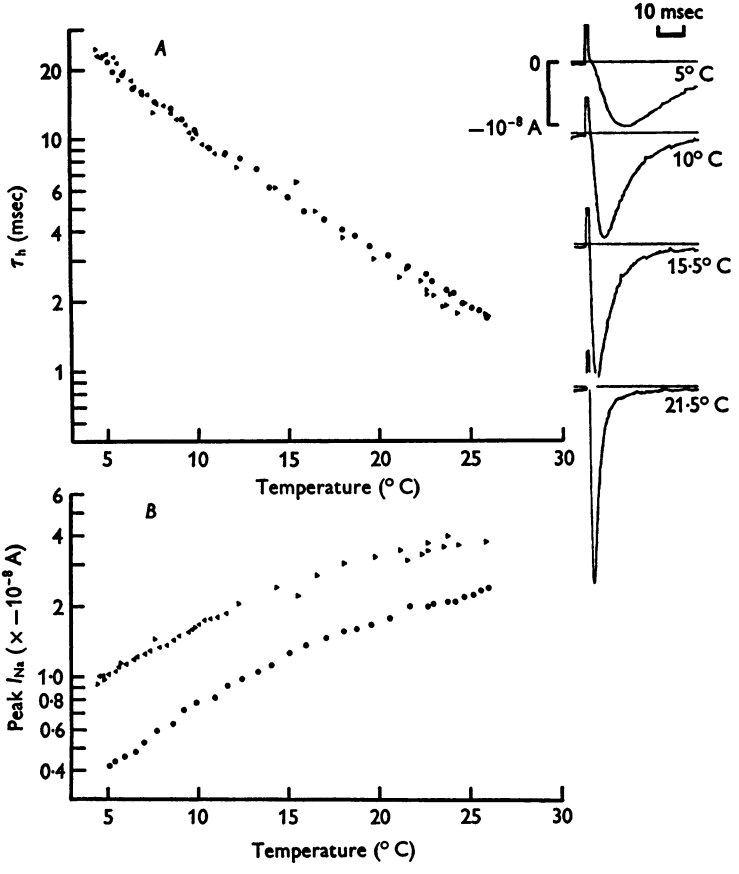

Fig. 11. Effects of changing the bath temperature upon Na currents at a fixed level of the membrane potential, −16 mV, in three eggs (EVC-37 (△), EVC-38 (●), EVC-39 (▲)). *A*: τ_h against temperature. The insets: samples of Na currents at four levels of the temperature in the egg, EVC-39. *B*: peak Na current against temperature.

Generally speaking, the process controlling the conductance change is known to have a temperature coefficient more than twice that of the maximum chord conductance. The fact supports the channel hypothesis for ionic conduction which assumes the separate processes between the

gating mechanism and the ion conducting mechanism through the molecular pore (Hille, 1970).

Steady-state current and inactivation of outward and inward rectifying conductances. Although the steady component of the membrane currents was very small in comparison with the transient current (Fig. 4*A*, filled triangles), the steady current also altered in connexion with the membrane potential, as illustrated in Fig. 4*B* with an expanded scale of the current. With hyperpolarization below −70 mV, the *V-I* relation showed an inward-going rectification and with depolarization beyond +20 mV a slight outward-going rectification was observed, as demonstrated previously with constant current stimulation. The inward-going rectification was identified as K anomalous rectification (Miyazaki *et al.* 1974*a*; Miyazaki *et al.* 1974*b*).

Both the large hyperpolarization below −120 mV and the large depolarization beyond +100 mV revealed characteristic activation and inactivation processes of inward and outward rectifying conductances respectively (Fig. 12 insets). The current traces with a depolarizing voltage step to +149 mV and with a hyperpolarizing voltage step to −186·5 mV both clearly show a decrease in the membrane currents or an inactivation of the conductances under the constant voltage condition. It was not clear whether the activation of both outward and inward rectifying conductances was time-dependent because the capacitative surge with the large voltage step did not allow the precise analysis of the initial portion of the current. The current traces with the voltage steps to −115 mV in Fig. 3*C* (arrow) and to +60 mV in Fig. 3*B* (arrow) suggested that there was some time delay for the activation of inward and maybe of outward rectifying conductances and there would be shorter delays with larger voltage steps. It should be noted that, in case of Fig. 3*B* at trace of +60 mV, the effect of the inactivation of the minor component of the inward currents can also cause the apparent time delay for the outward current. Similar time delay of the anomalous rectification of the striated muscle fibre has been reported by Almers (1971).

The graph of Fig. 12 illustrates both the steady-tate *V-I* curve (continuous line) and the initial *V-I* curve (interrupted line; arrows in the insets) measured with a voltage pulse of 400 msec duration. If there is a time delay for the activation, the initial means the measurement of the peak outward current within 10 msec after the voltage step. The *V-I* curves above −90 mV were obtained by the test pulse preceded by 400 msec prepulse to +20 mV with which both major and minor components of the transient inward currents were mostly inactivated. There was a clear activation of the outward-going rectification beyond +100 mV. The inactivation of both outward and inward rectifying conductances was

illustrated above +100 mV and below −120 mV respectively, as mentioned before. A similar inactivation of K outward rectifying conductances in the egg has been reported in the starfish oocyte (Miyazaki, Ohmori & Sasaki, 1974).

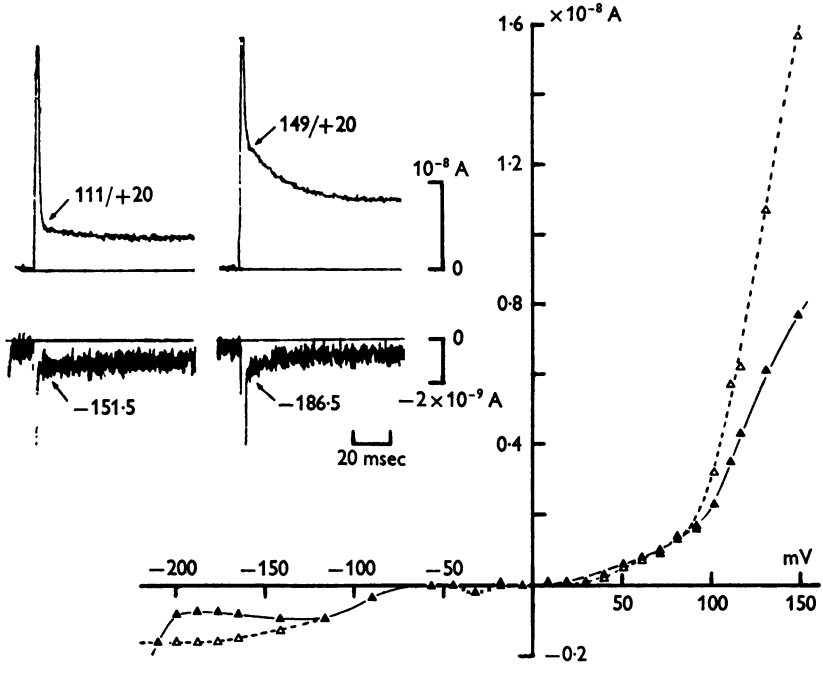

Fig. 12. The *V-I* relations of the initial transient (open triangle) and the steady-state currents (filled triangle) after the inactivation of both major and minor components of the inward currents (with +20 mV prepulse). Below −90 mV without prepulse, from an unfertilized egg (EVC-11). Temp. 13° C. The insets are samples of membrane currents with large depolarizing or hyperpolarizing pulses, of which the potential levels in mV were indicated by the figures on the traces. The measurements of the initial transient currents were illustrated by the arrows in the insets.

Discussion

A characteristic 'off response' found in the tunicate egg has been known to include both Na and Ca inward currents. In the present experiment, from the analysis of the membrane current by the voltage-clamp technique, it was concluded that the Na inward current of the egg was essentially identical with that of other excitable membranes. The reasons for this conclusion can be summarized as follows. (1) The egg Na inward current showed both activation and inactivation processes and those

kinetic parameters altered in correlation with the membrane potential in the same way as demonstrated in the common excitable membrane. (2) Li could be substituted for Na component of the inward current but neither Tris nor choline nor Cs could. (3) According to the results of the succeeding paper (Okamoto *et al.* 1976), Ca ions also could go through the egg Na channel as just proved in squid axons (Tasaki, Lerman & Watanabe, 1969; Baker, Hodgkin & Ridgway, 1971; Meves & Vogel, 1973). Although tetrodotoxin had no effect upon the egg Na current, it is still not unreasonable to identify the current as the one through Na channel since it has been reported that 'Na spikes' in the denervated muscle (Redfern & Thesleff, 1971) or the embryonic heart muscle (Ishima, 1968; Shigenobu & Sperelakis, 1971; Sperelakis & Shigenobu, 1972; MacDonald, Sachs & De Haan, 1973) or in the clone cultured rat myotube (Kidokoro, 1973) are all tetrodotoxin-resistant, and it is not strange that the undifferentiated egg cell membrane had tetrodotoxin-insensitive Na channel. All these facts, thus, indicate that Na channel which is characteristic of the axonal membrane is actually present in the egg cell membrane. In other words the Na channel has already been developed at the starting point of differentiation.

The Na inward current in standard ASW attained maximum at -30 to -25 mV and the peak value of the maximum inward current ranged from 1 to 3×10^{-8} A at the temperature of 14–15° C. Correspondingly, $\bar{g}_{Na}$ ranged from 0·2 to 0·7 μmho. Considering that the surface area of the unfertilized egg was 2×10^{-3} cm^2 (Miyazaki *et al.* 1974*a*), the maximum current density was $1{\cdot}5 \times 10^{-5}$ A/cm^2 and the maximum $\bar{g}_{Na}$ was 0·35 mmho/cm^2. Since the current density and the calculated chord conductance $\bar{g}_{Na}$ reported in the squid giant axons are 1·5 mA/cm^2 and 120 mmho/cm^2 respectively at the temperature of 6° C (Hodgkin & Huxley, 1952*d*), there would be more than a hundredfold difference of the channel densities between the egg membrane and the squid giant axon, if the permeability of each channel were the same between the two. However, there is another fact which suggests an alternative explanation of this difference of the $\bar{g}_{Na}$s. The Q_{10} of $\bar{g}_{Na}$ in the egg membrane was 2·0, while that of the squid axon is 1·2. According to Eyring's absolute rate theory on the ion permeation (Glasstone, Laidler & Eyring, 1941; Zwolinski, Erying & Reese, 1949), the larger activation enthalpy expected from the high Q_{10} will result in the lower permeability coefficient, assuming the same type of permeation barrier for Na channels of both egg cell and squid axon. Therefore, it is also possible to infer that the small $\bar{g}_{Na}$ of the egg membrane is not due to the low density of the channels on the membrane, but is caused by the low permeability in each channel.

Knowing the Q_{10}s for τ_m and τ_h in the squid axon to be 3·0, the kinetic

time constants τ_m and τ_h of Na current in the squid axons at 15° C can be calculated from Hodgkin and Huxley's data as about 0·2 msec and 0·5 msec respectively at a membrane potential of -30 mV (Hodgkin & Huxley, 1952*d*), while the egg Na current revealed τ_m of 2·2 msec and τ_h of 9·0 msec at the same potential level (Fig. 10*A*). There was ten- to twentyfold difference between the kinetic parameters of the tunicate egg and the squid in any range of the membrane potential. In addition to this quantitative difference of the kinetic parameters, we obtained slightly larger Q_{10}s of 4·0 to 3·0 for τ_m and τ_h in the egg membrane, while in the squid the Q_{10}s of τ_m and τ_h are about 3. If we adopted the absolute rate theory for description of the kinetic constants of the gating mechanism in the egg Na current, as proposed by Tsien & Noble (1969), the larger Q_{10} may be attributed to the higher activation enthalpy of the gating process. At the present moment, we have no explanations about the nature of the quantitative difference of the gating speed between eggs and axons since the molecular mechanisms of the gating process are not known precisely yet.

Characterization of the Ca current, which was described as a minor component of the inward current in the present paper, will be given in a succeeding paper (Okamoto *et al.* 1976) and it will be concluded that the egg Ca channel is also identical with the Ca channel known in crustacean muscle membrane.

Although the egg K current was much less dominant in comparison with Na inward current, the previous paper demonstrated clearly K anomalous rectification in the egg membrane (Miyazaki *et al.* 1974*a*) and the present voltage-clamp experiment confirmed it. The outward rectifying conductance was scarcely found in the potential range below $+25$ mV in the ASW of standard Ca concentration of 10 mM. Therefore, in the egg membrane, it may be concluded that K outward rectification is extremely rare. However, there would be another possibility that K outward rectifying channels in the egg might have an extremely positive critical membrane potential for their activation, as inferred from Fig. 12. In either case, it is fairly reasonable to consider that four ionic channels for Na, Ca, K inward rectifying, and K outward rectifying conductances all exist and only Na and Ca channels are relatively dominant in the egg cell membrane where developmental or differentiation processes initiate.

Since Hodgkin & Huxley proposed the independent and separate conducting paths for Na and K, concerning the production of the action potential (Hodgkin & Huxley, 1952*d*), much evidence has been accumulated for the proposal. (1) Existence of specific and selective effects of pharmacological agents, such as tetrodotoxin or tetraethylammonium upon the several conducting paths or channels (Narahashi *et al.* 1964; Nakamura *et al.* 1965; Tasaki & Hagiwara, 1957; Armstrong & Binstock,

1965; Hille, 1970). (2) Differential effects of several physicochemical agents, such as temperature, proteolytic enzymes, pH, divalent ion concentration in the bath solution upon the gating and conducting mechanisms of ionic paths or channels (Tasaki & Takenaka, 1964; Armstrong, Bezanilla & Rojas, 1973; Hille, 1968; Frankenhaeuser & Hodgkin, 1957; Chandler *et al.* 1965). (3) Presence of antibiotics which have been considered to form ion conducting channels through bimolecular lipid membrane (Mueller & Rudin, 1963; Hladky & Haydon, 1970; Urry, Goodall, Glickson & Mayers, 1971; Krasne, Eisenman & Szabo, 1971).

A series of our experiments on the tunicate egg and embryo suggested an importance of quantitative alteration of relative dominancy among several ion permeating systems rather than qualitative alteration of the mode of the ion permeation during the embryonic development since the modes of ion permeation in the egg cell membrane were found to be identical with those of the differentiated excitable membrane. Our studies thus support the proposal of the existence of discrete entities for the ion conductive paths. In other words, it can be said that the findings in the present experiments supported the 'channel' hypothesis from the ontogenic aspects.

We would like to thank Professor A. Takeuchi for useful comments on this manuscript. This investigation was supported by a research grant from the Educational Ministry of Japan. We acknowledge the marine biological laboratory of Tohoku University at Asamushi, Miyagi prefectual fisheries experimental station at Kesennuma, Otaru city Aquarium and Wakkanai City Aquarium in Hokkaido for collecting materials.

REFERENCES

ALMERS, W. (1971). The potassium permeability of frog muscle membrane. Ph.D. Thesis Dissertation, University of Rochester, Rochester, N.Y.

ARMSTRONG, C. M., BEZANILLA, F. & ROJAS, E. (1973). Destruction of sodium conductance inactivation in squid axons perfused with pronase. *J. gen. Physiol.* **62**, 375–391.

ARMSTRONG, C. M. & BINSTOCK, L. (1965). Anomalous rectification in the squid giant axon injected with TEA chloride. *J. gen. Physiol.* **48**, 859–872.

BAKER, P. F., HODGKIN, A. L. & RIDGWAY, E. B. (1971). Depolarization and calcium entry in squid giant axons. *J. Physiol*, **218**, 709–755.

CHANDLER, W. K., HODGKIN, A. L. & MEVES, H. (1965). The effect of changing the internal solution on sodium inactivation and related phenomena in giant axons. *J. Physiol.* **180**, 821–836.

CHANDLER, W. K. & MEVES, H. (1965). Voltage clamp experiments on internally perfused giant axons. *J. Physiol.* **180**, 788–820.

CHANDLER, W. K. & MEVES H. (1970). Slow changes in membrane permeability and long-lasting action potentials in axons perfused with fluoride solutions. *J. Physiol.* **211**, 707–728.

COLE, K. S. (1968). *Membranes, Ions and Impulses*, pp. 274–291. Berkeley: University of California Press.

DODGE, F. A. & FRANKENHAEUSER, B. (1958). Membrane currents in isolated frog nerve fibre under voltage clamp conditions. *J. Physiol.* **143**, 76–90.

DODGE, F. A. & FRANKENHAEUSER, B. (1959). Sodium currents in the myelinated nerve fibre of *Xenopus laevis* investigated with the voltage clamp technique. *J. Physiol.* **148**, 188–200.

EINSEBERG, R. S. & ENGEL, E. (1970). The spatial variation of membrane potential near a small source of current in a spherical cell. *J. gen. Physiol.* **55**, 736–757.

FRANKENHAEUSER, B. (1959). Steady state inactivation of sodium permeability in myelinated nerve fibres of *Xenopus laevis*. *J. Physiol.* **148**, 671–676.

FRANKENHAEUSER, B. (1960). Quantitative description of sodium current in myelinated nerve fibres of *Xenopus laevis*. *J. Physiol.* **151**, 491–501.

FRANKENHAEUSER, B. & HODGKIN, A. L. (1957). The action of calcium on the electrical properties of squid axons. *J. Physiol.* **137**, 218–244.

FRANKENHAEUSER, B. & MOORE L. E. (1963*a*). The effect of temperature on the sodium and potassium permeability changes in myelinated nerve fibres of *Xenopus laevis*. *J. Physiol.* **169**, 431–437.

FRANKENHAEUSER, B. & MOORE L. E. (1963*b*). The specificity of the initial current in myelinated nerve fibres of *Xenopus laevis*. *J. Physiol.* **169**, 438–444.

GLASSTONE, S., LAIDLER, K. J. & EYRING H. (1941). *The Theory of Rate Processes*. New York: McGraw Hill.

HAGIWARA, S. & NAKA, K. (1964). The initiation of spike potential in Barnacle muscle fibers under low intracellular Ca^{++}. *J. gen. Physiol.* **48**, 141–162.

HILLE, B. (1967), The selective inhibition of delayed potassium currents in nerve by tetraethyl ammonium ion. *J. gen. Physiol.* **50**, 1287–1302

HILLE, B. (1968). Charges and potentials at the nerve surface: divalent ions and pH. *J. gen. Physiol.* **51**, 221–236.

HILLE, B. (1970). Ionic channels in nerve membranes. *Prog. Biophys. molec. Biol.* **21**, 1–32.

HILLE, B. (1971). Voltage clamp studies on myelinated nerve fibres. In *Biophysics and Physiology of Excitable Membrane*, ed. ADELMAN, W. J., pp. 230–246.

HILLE, B. (1972). The permeability of the sodium channel to metal cations in myelinated nerve. *J. gen. Physiol.* **59**, 637–658.

HLADKY, S. B. & HAYDON, D. A. (1970). Discreteness of conductance change in bimolecular lipid membranes in the presence of certain antibiotics. *Nature, Lond.* **225**, 451–453.

HODGKIN, A. L. (1958). Ionic movements and electrical activity in giant nerve fibres. *Proc. R. Soc.* B **148**, 1–37.

HODGKIN, A. L. & HUXLEY, A. F. (1952*a*). Current carried by sodium and potassium ions through the membrane of the giant axon of *Loligo*. *J. Physiol.* **116**, 449–472.

HODGKIN, A. L. & HUXLEY, A. F. (1952*b*). The components of membrane conductance in the giant axon of *Loligo*. *J. Physiol.* **116**, 473–496.

HODGKIN, A. L. & HUXLEY, A. F. (1952*c*). The dual effect of membrane potential on sodium conductance in the giant axon of *Loligo*. *J. Physiol*, **116**, 497–506.

HODGKIN, A. L. & HUXLEY, A. F. (1952*d*). A quantitative description of membrane current and its application to conduction and excitation in nerve. *J. Physiol.* **117**, 500–544.

HODGKIN, A. L., HUXLEY, A. F. & KATZ, B. (1952). Measurement of current voltage relations in the membrane of the giant axon of *Loligo*. *J. Physiol.* **116**, 424–448.

HODGKIN, A. L. & KATZ, B. (1949). The effect of sodium ions on the electrical activity of the giant axon of the squid. *J. Physiol.* **108**, 37–77.

ISHIMA, Y. (1968). The effect of tetrodotoxin and sodium substitution on the action potential in the course of development of the embryonic chicken heart. *Proc. Japan. Acad.* **44**, 170–175.

KIDOKORO, Y. (1973). Development of action potentials in a clonal rat skeletal muscle cell line. *Nature, New Biol.* **241**, 158–159.

KOPPENHÖFER, E. & SCHMIDT, H. (1968). Die Wirkung von Skorpiongift auf die Ionenstrome des Ranvierschen Schnurrings. I. Die Permeabilitäten P_{Na} und P_K. *Pflügers Arch. ges. Physiol.* **303**, 133–149.

KRASNE, S., EISENMAN, G. & SZABO, G. (1971), Freezing and melting of lipid bilayers and the mode of action of nonaction valinomycin and gramicidin. *Science, N.Y.* **174**, 412–415.

MACDONALD, T. F., SACHS, H. G. & DE HAAN, R. L. (1973). Tetrodotoxin desensitization in aggregate of embryonic chick heart cells. *J. gen. Physiol.* **62**, 286–302.

MEVES, H. & VOGEL, W. (1973). Calcium inward currents in internally perfused giant axons. *J. Physiol.* **235**, 225–265.

MIYAZAKI, S., OHMORI, H. & SASAKI, S. (1974). K rectifications of the starfish oocyte membrane and their changes during maturation. *J. Physiol.* **246**, 55–78.

MIYAZAKI, S., TAKAHASHI, K. & TSUDA K. (1972). Calcium and sodium contributions to regenerative responses in the embryonic excitable cell membrane. *Science, N.Y.* **176**, 1441–1443.

MIYAZAKI, S., TAKAHASHI, K. & TSUDA, K. (1974*a*). Electrical excitability in the egg cell membrane of the tunicate. *J. Physiol.* **238**, 37–54.

MIYAZAKI, S. TAKAHASHI, K., TSUDA, K., & YOSHII, M. (1974*b*). Analysis of non-linearity observed in the current–voltage relation of the tunicate embryo. *J. Physiol.* **238**, 55–77.

MOORE, J. W., ANDERSON, N. C., BLAUSTEIN, M. P., TAKATA, M., LETTVIN, J., PICKARD, W. F., BERNSTEIN, T. & POOLER, J. (1966). Alkali cation specificity of squid axon membrane. *Ann. N.Y. Acad. Sci.* **137**, 818–829.

MOORE, J. W., BLAUSTEIN, M. P., ANDERSON, N. C. & NARAHASHI, T. (1967). Basis of tetrodotoxin's selectivity in blockage of squid axons. *J. gen. Physiol.* **50**, 1401–1411.

MOORE, J. W. & COLE, K. S. (1963). Voltage clamp techniques. In *Physical Techniques in Biological Research. VI*, ed. NASTUK, W. L. New York: Academic Press.

MOORE, L. E. (1971). Effect of temperature and calcium ions on rate constants of myelinated nerve. *Am. J. Physiol.* **221**, 131–137.

MUELLER, P. & RUDIN, D. O. (1963). Induced excitability in reconstituted cell membrane structure. *J. theor. Biol.* **4**, 268–280.

NAKAMURA, Y., NAKAJIMA, S. & GRUNDFEST, H. (1965). The action of tetrodotoxin on electrogenic components of squid giant axons. *J. gen. Physiol.* **48**, 985–996.

NARAHASHI, T., MOORE, J. W. & SCOTT, W. R. (1964). Tetrodotoxin blockage of sodium conductance increase in lobster giant axons. *J. gen. Physiol.* **47**, 965–974.

OKAMOTO, H., TAKAHASHI, K. & YOSHII, M. (1976). Two components of the Ca current of the egg cell membrane of the tunicate. *J. Physiol.* (in the Press).

OVERTON, E. (1902). Beitrage zur allgemeinen Muskel- und Nervenphysiologie. *Pflügers Arch. ges. Physiol.* **92**, 346–386.

REDFERN, P. & THESLEFF, S. (1971). Action potential generation in denervated rat skeletal muscle. II. The action of tetrodotoxin. *Acta physiol. scand.* **82**, 70–78.

ROJAS, E. & ATWATER, I. (1967). Effect of tetrodotoxin on the early outward currents in perfused giant axons. *Proc. natn. Acad. Sci. U.S.A.* **57**, 1350–1355.

SCHAUF, C. L. (1973). Temperature dependence of the ionic current kinetics of *Myxicola* giant axons. *J. Physiol.* **235**, 197–205.

SHIGENOBU, K. & SPERELAKIS, N. (1971). Development of sensitivity to tetrodotoxin of chick embryonic hearts with age. *J. molec. cell. Cardiol.* **3**, 271–286.

SPERELAKIS, N. & SHIGENOBU, K. (1972). Changes in membrane properties of chick embryonic hearts during development. *J. gen. Physiol.* **60**, 430–453.

TAKAHASHI, K., MIYAZAKI, S. & KIDOKORO, Y. (1971). Development of excitability in embryonic muscle cell membranes in certain tunicates. *Science, N.Y.* **171**, 415–418.

TASAKI, I. & HAGIWARA, S. (1957). Demonstration of two stable potential states in the squid giant axon under tetraethylammonium. *J. gen. Physiol.* **40**, 859–885.

TASAKI, I., LERMAN, L. & WATANABE, A. (1969). Analysis of excitation process in squid giant axons under bi-ionic conditions. *Am. J. Physiol.* **216**, 130–138.

TASAKI, I. & TAKENAKA, T. (1964). Effects of various potassium salts and proteases upon excitability of intracellularly perfused squid giant axons. *Proc. natn. Acad. Sci. U.S.A.* **52**, 804–810.

TSIEN, R. W. & NOBLE, D. (1969). A transition state theory approach to the kinetics of conductance changes in excitable membranes. *J. membrane Biol.* **1**, 248–273.

URRY, D. W., GOODALL, M. C., GLICKSON, J. P. & MAYERS, D. F. (1971). The gramicidin A transmembrane channel: characteristics of head to head dimerized π (L,D) helics. *Proc. natn. Acad. Sci. U.S.A.* **68**, 1907–1911.

ZWOLINSKI, B. J., EYRING, H. & REESE, C. E. (1949). Diffusion and membrane permeability. *J. phys. Colloid Chem.* **53**, 1426–1453.